Microchim Acta (2015) 182:1643–1651
DOI 10.1007/s00604-015-1489-5

ORIGINAL PAPER

Zinc oxide nanoparticle-enhanced ultrasensitive chemiluminescence immunoassay for the carcinoma embryonic antigen

Souvik Pal[1] · **Sunil Bhand**[1]

Received: 23 December 2014 / Accepted: 30 March 2015 / Published online: 18 April 2015

Abstract An ultrasensitive enzyme-linked immunosorbent assay (ELISA) is reported for the determination of carcinoma embryonic antigen (CEA) in human serum. It was realized using a microplate reader using a 384-well plate. Monoclonal antibody (Ab) against CEA (1° Ab) acting as the capture probe was immobilized on zinc oxide nanoparticles (ZnO-NPs) in the form of self-assembled monolayers (SAMs). CEA captured by 1° Ab was quantified using a sandwich ELISA wherein a polyclonal second antibody against CEA (2° Ab) was used for detection and quantified using an HRP-labeled secondary antibody (3° Ab). The ZnO-NPs-CEA capture probe was deposited on the bottom of the wells in order to enhance capture of CEA. A 3-fold enhancement in the chemiluminescence (CL) signal of luminol is found (compared to a conventional ELISA). CEA can be quantified by this method in concentrations as low as 1 $pg \cdot mL^{-1}$. The upper limit of detection is 20 $ng \cdot mL^{-1}$. The use of ZnO-NPs also imparts improved thermal stability. When stored at 4 °C in phosphate-buffered saline of pH 7.4, the probe displays stability of up to 30 days.

Keywords Carcinoma embryonic antigen · Zinc oxide · Self-assembled monolayer · Sandwich ELISA · Serum · Chemiluminescence

Electronic supplementary material The online version of this article (doi:10.1007/s00604-015-1489-5) contains supplementary material, which is available to authorized users.

✉ Sunil Bhand
sunil17_bhand@yahoo.com; sunilbhand@goa.bits-pilani.ac.in

[1] Biosensor Lab. Department of Chemistry, BITS, Pilani –KK Birla Goa Campus, Goa 403726, India

Introduction

The determination of tumor makers is one of the important prognostic factors in clinical research and diagnosis. Sensitive detection of the biomarkers is vitally important for timely diagnosis and treatment of early stage cancers, which largely determines the survival rate of cancer patients [1, 2]. Immunoassay is an easy and low-cost method in the detection of antigen or its specific antibody in clinical diagnostics [3]. Because of its adaptability, simplicity and sensitivity, enzyme-linked immunosorbent assay (ELISA) is one of the most extensively used analytical techniques in clinical research [4, 5]. Owing to their high sensitivity, preclusion of radiation damage and relatively simple instrumentation, chemiluminescence (CL) immunoassays have been commonly applied in the routine clinical analysis [6]. The sensitivity of conventional polystyrene plate ELISA for subsequent antibody-antigen recognition and binding sometimes have failed due to the low surface-to-volume ratio of the plate and the random orientation of the adsorbed Ab [7]. The concentrations of cancer bio-markers are extremely low, i.e., $ng \cdot mL^{-1}$ or lower in vivo [8, 9]. Therefore, developing miniaturized ELISA for improved sensitivity, lower limit of detection and reproducibility is a paramount need in routine diagnosis. Sandwich-type immuno-sensors and immunoassay methods were developed for detection of Ag with more than one epitope due to the use of matched antibodies. High-affinity antibodies and appropriate labels were usually employed for the amplification of detectable signal. Nanoparticles (NPs) have been used in sandwich-type immuno-sensors and immunoassays as innovative and powerful novel labels. Their properties can be controlled and tailored in a very predictable manner to meet the requirements of specific applications [4].

Carcinoma embryonic antigen (CEA), a polysaccharide–protein complex, is one of the most studied tumor markers due to its association with liver, colon, colorectal and breast cancer and existence in endoblast origin digestive system cancer [10]. Higher levels of CEA in serum were reported for individuals with colorectal, gastric, pancreatic, lung, and breast carcinomas, as well as individuals with medullary thyroid carcinoma than healthy individuals [11, 12]. The reported concentrations of CEA are 2.5 $ng \cdot mL^{-1}$ for non-smokers and 5.0 $ng \cdot mL^{-1}$ for smokers, respectively [13]. Thus, accurate determination of CEA is of significance for monitoring and prognosis of disease recurrence. The long-term survival of cancer patients can be improved by considering the levels of CEA in human organism, which reflects the disease progression or regression status [14]. As a result, there is an immense need for a sensitive immunoassay technique to detect a sub-nanogram per milliliter level.

Recently, we have demonstrated a novel enzymatic nanobiosensor for choline using ZnO nanorods (ZnONR) stabilized using 16-phosphonohexadecanoic acid (16-PHA) [15]. Herein, we report the development of ultra-sensitive NPs based ELISA for detection of CEA levels in human serum using zinc oxide nanoparticles based CEA probe (ZnO-NPs-CEA). The develop ZnO-NPs-CEA assay exhibited enhanced signal intensity, broader linear range and thermal stability over the conventional ELISA. A significant enhancement in sensitivity (about two fold per decade) was achieved with a lower limit of detection 1 $pg \cdot mL^{-1}$. The use of 1° Ab coupled ZnO-NPs as affinity capture material using a miniaturized microwell plate platform for CEA gave better efficiency of capture and stability over reported materials (Table 1).

Experimental

The materials and apparatus used are described in the Electronic Supplementary Material (ESM).

Preparation of buffers and samples

For coating purpose, a 50 mM carbonate buffer (CB) was prepared. The pH was adjusted to 9.6. As CB can change the composition over time, it was made fresh each time. 10 mM phosphate-buffered saline (PBS, pH 7.4) containing 137 mM NaCl, 2 mM KCl was used for incubation and washing purpose. Another washing buffer (PBST) was made by adding 0.05 % Tween 20 (*v/v*) in PBS. All buffer solutions were stored at 4 °C when not in use. The blocking solution was prepared by adding 2.5 % (*w/v*) BSA to PBS.

The stock 1° Ab (2 $mg \cdot mL^{-1}$) was diluted in 10 mM PBS to the final concentration (0.2 $\mu g \cdot mL^{-1}$). The stock 2° Ab (2 $mg \cdot mL^{-1}$) specifically to 1° Ab was diluted to 0.5 $\mu g\ mL^{-1}$ as indicated by manufacturer's protocol. 1 μL of the stock solution of 3° Ab-HRP (2 $mg \cdot mL^{-1}$) was diluted with 50 μL of de-ionized water. From the 1:50 dilution, working 3° Ab-HRP solution was prepared prior to the experiment by diluting 1:100, 1:500 and so on in PBS. The standard serum was used without any further dilution. CEA spiked serum solutions were prepared by standard addition method in the range 20–0.001 $ng \cdot mL^{-1}$.

CEA analysis using conventional ELISA

All liquid pipetting was performed using Eppendorf multichannel pipette in automatic mode. Conventional sandwich ELISA was performed in 384 microwell plate. An optimized 1° Ab was diluted to 0.2 $\mu g \cdot mL^{-1}$ in CB. Diluted 1° Ab (40 μL) was coated in each microwell. The plate was covered and kept at room temperature for 3 h. Each microwell was washed three times with 60 μL PBS. The remaining protein binding sites in the coated wells were blocked by adding 20 μL of 2.5 % BSA blocking solution for 1 h at room temperature. The plate was washed with 50 μL PBST. Following this step, CEA spiked serum samples in the range 20–0.001 $ng \cdot mL^{-1}$ were added as 20 μL in each well. The plate was incubated for about 2 h at room temperature. The unbound CEA antigen was removed by washing three times with 60 μL PBS. Then 1:1 mixture of optimized 2° Ab and 3° Ab-HRP was prepared. The excess label was removed by washing PBS. The final solution was added as 30 μL in each well. The plate was kept for 2 h at room temperature. The excess label was removed by washing three times with 60 μL PBS. The chemiluminescence (CL) substrate (1 μL of 0.05 M H_2O_2+ 4 μL of 0.5 mM luminol) was added. The signal intensity was kinetically measured at the steady state and stability was found after 30 min.

Construction of ZnO-NPs – CEA capture probe

Surface modification The development of CEA capture probe was based on the efficient immobilization of very specific anti-CEA 1° Ab through carboxy terminated SAMs on ZnO-NPs. The glass container used for monolayer preparation was cleaned with Piranha solution (a mixture of 98 % H_2SO_4 and 30 % H_2O_2, 7:3, *v/v*; caution: piranha solution reacts exothermally and strongly reacts with organics) for 1 h and rinsed exhaustively with de-ionized (DI) water and ethanol. 16-PHA modified ZnO-NPs were prepared as described in our previous report [15]. Briefly, 3 mg of ZnO-NPs was dispersed in 0.5 mM ethanolic solution of 16-PHA. The resulted suspension of particles was mechanically stirred for 72 h for SAMs formation.

Covalent coupling of 1° Ab onto ZnO-NPs For antibody immobilization, the carboxylic acid-terminated SAMs were modified using an aqueous equimolar solution of 100 mM

Table 1 Comparison of present assay with earlier reported immunosensors

Sensor configuration	Transduction principle	Linear detection range ($ng \cdot mL^{-1}$)	Limit of detection ($pg \cdot mL^{-1}$)	References
ZnO-NPs coupled 1° Ab on 384 microwell plate	Sandwich CL immunoassay	0.001 – 20	1.0	This work
Conventional ELISA	Sandwich CL immunoassay	0.01 – 10	10	This work
Ab2-PdPt-Thi/Fc as probes	Electrochemical	0.05 – 200	1.4	[25]
Conjugated biotinylated anti-CEA Ab on streptavidine coated superparamagnetic beads	Sandwich CL immunoassay	0.005 – 50	5.0	[3]
Fe_3O_4@C@CdTe QDs composite with CEA-mAb1 and the ZnO NWs	Sandwich fluorometric immunoassay	0.005 – 100	1.6	[26]
ZnONPs and glucose oxidase decorated graphene	Sandwiched luminol electrochemiluminescence immunosensing	0.01 – 80	3.3	[27]

EDC /100 mM NHS for 2 h at room temperature. The resultant NHS ester monolayers were reacted in room temperature for 3 h in 1:1 solution of 1° Ab (0.2 $\mu g \cdot mL^{-1}$) and CB. The 1° Ab coated ZnO-NPs (1° Ab-ZnO-NPs) were washed with PBS.

ZnO-NPs based ELISA The ZnO-NPs-CEA capture probe was coated in the bottom of the 384 well plates for enhanced capture of CEA antigen. The remaining protein binding sites in the ZnO-NPs were blocked by adding 20 μL of 2.5 % BSA blocking solution for about 1 h at room temperature. After washing step by PBST, CEA spiked serum samples (20 μL in each well) were incubated for 2 h at room temperature. The particles were washed again with 50 μL PBS to remove unbound CEA. The 2° Ab (15 μL) was incubated at room temperature for 2 h with the particles. Finally, for CL measurements, 15 μL of 3° Ab-HRP (1:2000) was incubated at room temperature for 1 h with the particles. The excess label was removed by washing with PBS. The CL substrate (1 μL of 0.05 M H_2O_2+4 μL of 0.5 mM luminol) was added. The signal intensity was kinetically measured at the steady state, and stability was found after 25 min.

The hybrid- immuno assay was realized in 384 micro well plates using anti CEA- monoclonal antibody (1° Ab) immobilized on ZnO-NPs via self-assembled monolayer as capture probes. The captured antigen was quantified using sandwich ELISA wherein a polyclonal anti CEA 2° Ab was used for detection and quantified using an enzyme labeled secondary antibody 3° Ab. The schematic of the detection procedure is shown in Fig. 1.

Results and discussions

Choice of materials

Bio-sensing techniques commonly rely upon the use of bio-functionalized NPs, inorganic-biological hybrid NPs, and signal tag-doped NPs [16]. The enormous signal enhancement associated to the use of NPs labels, and with the formation of nanoparticle-antibody-antigen assemblies provides the basis for sensitive detection of disease-related proteins or biomolecules [17]. Hybrid approaches involve noble metal NPs, carbon NPs, semiconductor NPs, metal oxide nano-structures, and hybrid nano-structures. Nano-structured metal oxides of zirconium, titanium, cerium, tin and zinc have gained much attention in bio-sensor and immuno-sensor application owing to their large surface to volume ratio, high surface reaction activity, high catalytic efficiency, and strong adsorption ability.

Choice of nano-structured oxide materials is crucial for immobilization of the desired biomolecule. The interface formed due to binding between an oxide nano-material and a

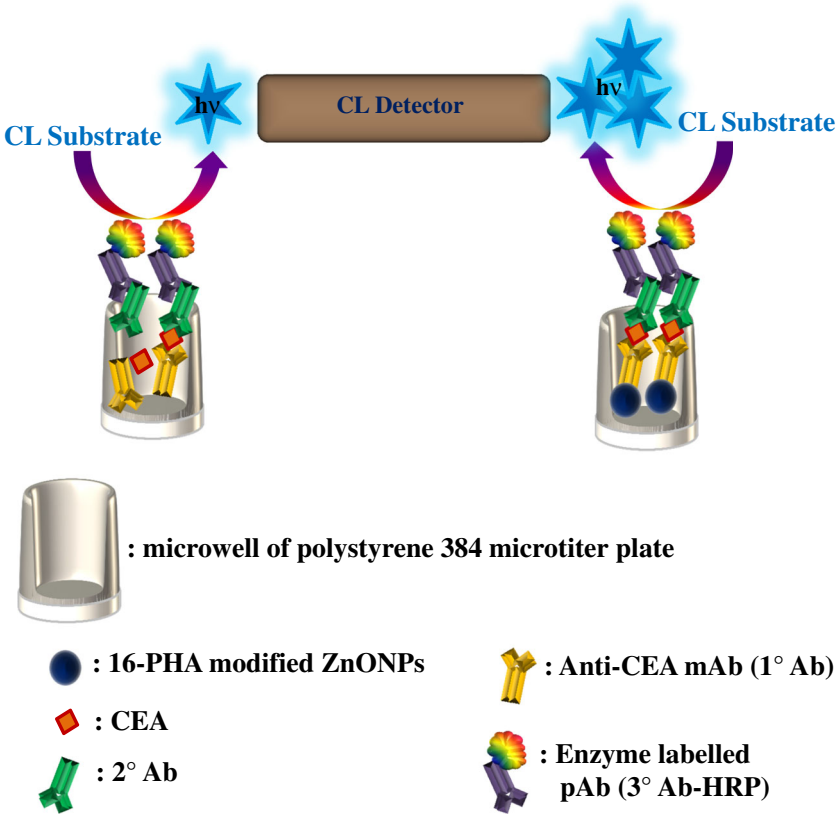

Fig. 1 Schematic representation of the CEA recognition process

biomolecule can influence the performance of an immunosensor. The formation and properties of a nano – bio interface depends upon the nature of nano-structure parameters like surface charge, valence/conductance states, functional groups, physical states and hygroscopic nature [16].

Among the other reported metal oxide nano-structures, ZnO is well known for its biocompatibility, high specific surface area, chemical and photochemical stability, excellent light transmission, strong electrochemical and electron communication response and lack of toxicity [18]. Owing to its non-toxicity, good bio-compatibility and high chemical stability, ZnO was used widely in construction of bio-sensors [19]. The high isoelectric point of ZnO, which is about 9.5, plays an important role in biological pH [20]. Due to lowering of isoelectric point in biological pH, the surface of ZnO has a positive charge; protein with a low isoelectric point (in case of CEA is 4.7) can be immobilized on it by an electrostatic force [21]. Furthermore, it was observed that ZnO-NPs based luminol-H_2O_2 system can also enhance the CL signals. The CL enhancement of ZnO-NPs may be attributed to the catalysis of ZnO-NPs on the radical generation and electron-transfer processes during the luminol CL reaction [22]. These observations indicate that the ZnO-NPs promote electron transport and thus improved the sensitivity and selectivity as compared to conventional ELISA.

Characterization of ZnO-NPs – CEA probe

Affinity analysis of ZnO-NPs – CEA capture probe

Real time binding analysis using QCM was performed to confirm the CEA binding on the 16-PHA modified ZnO surface. The functionalized quartz crystal ZnO-16PHA (10 MHz, non-bonded) was placed in a plexiglass flow cell in static mode, sandwiched between two O-rings and connected to the frequency-measuring unit. The direct mass change was recorded using Voltascan 5 software. The data was plotted and presented as Fig. 2a. The 16-PHA modified ZnO quartz crystals were prepared for the QCM study as described earlier. The binding of 1° Ab, CEA, 2° Ab and 3° Ab-HRP were performed in static mode using the optimized condition as earlier. The mass change was recorded after each step. The increasing change in mass confirms the stepwise binding of (i) 1° Ab (anti-CEA), (ii) CEA-Ag, (iii) 2° Ab and (iv) 3° Ab-HRP. The 1° Ab attached on SAMs modified ZnO crystal showed the initial mass of 121 ng. Subsequent mass changes of 91 ng, 303 ng, 331 ng and 223 ng were observed for the attachment of 1° Ab, CEA, 2° Ab and 3° Ab-HRP respectively as shown in Fig. 2a. Upon using 2° Ab for CEA recognition, a mass change of 28 ng was observed. Whereas, with the 3° Ab as recognition probe, a negligible mass change (0.048563 ng).was observed.

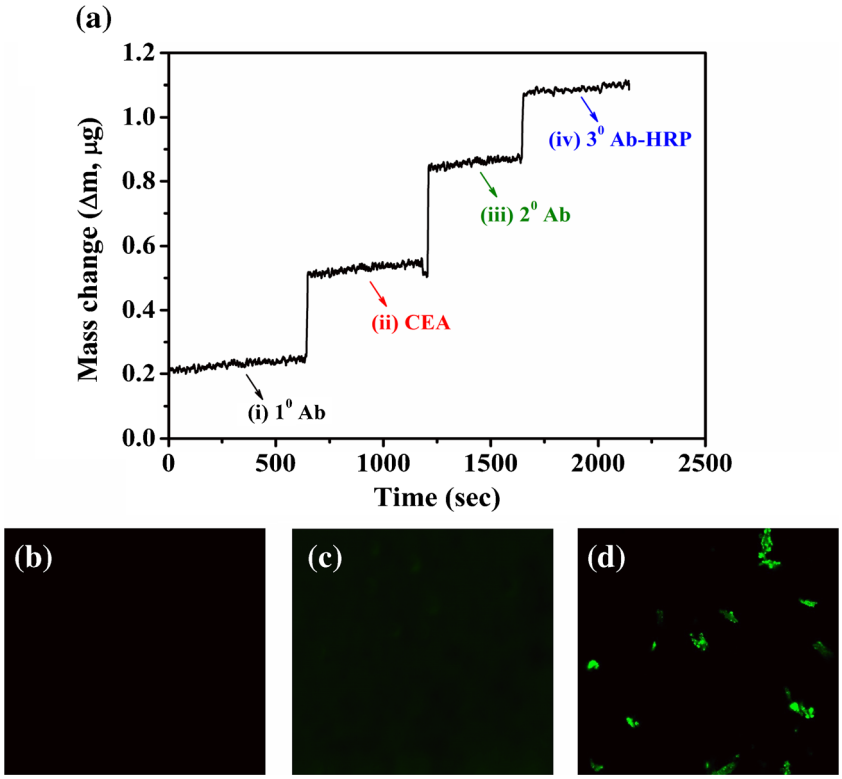

Fig. 2 **a** Stepwise mass change response on SAMs modified ZnO crystal after the attachment of (i) 1° Ab (anti-CEA); (ii) CEA-Ag; (iii) 2° Ab, and (iv) 3° Ab-HRP; Fluorescence image of **b** reference 1° Ab-ZnO-NPs without 3° Ab-FITC, **c** sample 1° Ab-ZnO-NPs directly coupled with labelled 3° Ab (3° Ab-FITC), **d** sample 1° Ab-ZnO-NPs coupled with unlabelled 2° Ab and 3° Ab-FITC at 20× magnification; incubated with 3° Ab-FITC (1:8000) (λ_{ex} 480 nm / λ_{em} 520 nm)

Thus, it can be concluded that 2° Ab was working as recognition of CEA. Further, the significant mass change observed for CEA capture using the ZnO-16PHA-anti CEA provided a strong evidence of the enhanced surface to volume ratio available for successful construction of a ZnO-NPs based immunosensor.

Fluorescence binding studies of 3° probe

The specificity of the 3° Ab was further confirmed by fluorescence microscopy. Microscopy slides were prepared as (a) reference 1° Ab-ZnO-NPs without 3° Ab-FITC, (b) sample 1° Ab-ZnO-NPs directly coupled with labelled 3° Ab (3° Ab-FITC) and (c) sample 1° Ab-ZnO-NPs coupled with unlabelled 2° Ab and 3° Ab-FITC. During measurement, suspended 1° Ab-ZnO-NPs (3 μL) were spotted onto three glass slide that were dried by keeping in a humidity chamber at room temperature. One of the spotted 1° Ab-ZnO-NPs glass microscopy slides was named as reference (1° Ab-ZnO-NPs without 3° Ab-FITC). Another glass slide among the three was incubated with 3° Ab-FITC (1:8000) for 2 h at room temperature in dark. This slide was designated as sample (1° Ab-ZnO-NPs directly coupled with labelled 3° Ab). The remaining glass slide was incubated with 2° Ab (15 μL) at room temperature for 2 h. Finally, for fluorescence measurements, 15 μL of 3° Ab-FITC (1:8000) was incubated at room temperature for 2 h in dark. This slide was also assigned as sample (1° Ab-ZnO-NPs coupled with unlabelled 2° Ab and 3° Ab-FITC). Before excitation the sample slides were rinsed with 10 mM PBS to remove unbound 3° Ab-FITC. The reference 1° Ab-ZnO-NPs without 3° Ab-FITC and sample 1° Ab-ZnO-NPs directly coupled with labeled 3° Ab (3° Ab-FITC) showed negligible fluorescence signal as the binding is non-specific (Fig. 2b and c). The binding between 1° Ab on ZnO-NPs and 1° Ab specific unlabelled 2° Ab, 3° Ab-FITC were demonstrated by a bright fluorescence signal from the agglomerated spots (Fig. 2d). These observations proved that the 1° Ab on ZnO-NPs preserved the excellent biological recognition of antibody to their targets.

Development of immunoassay

Optimization of experimental conditions

The optimum results for the ionic strength and pH of PBS were found at 10 mM, pH 7.4 (Supplementary Figure S1 and S2). It was found that a 3° Ab-HRP dilution of 1:2000 produced better signal intensity against 1° Ab (0.2 $\mu g \cdot mL^{-1}$) (Supplementary Figure S3). Further, the amount of ZnO-NPs – CEA probe particles was also optimized as 2 $mg \cdot mL^{-1}$, having maximum signal intensity (Supplementary Figure S4).

Thermal stability of ZnO-NPs – CEA probe

The thermal stability was compared for the 1° Ab coupled of ZnO-NPs and 1° Ab immobilized on the microwell plate. The

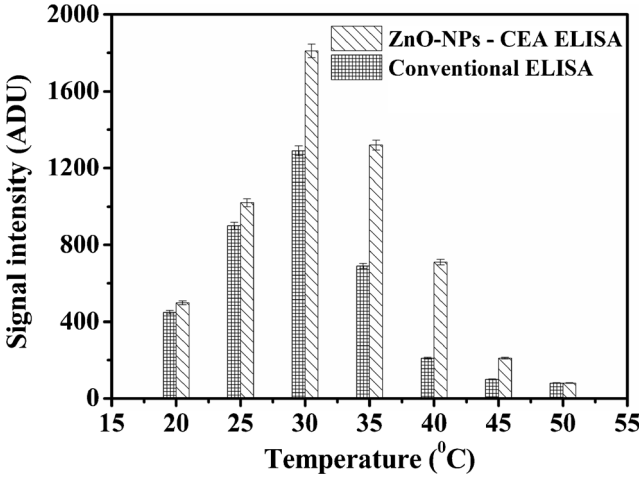

Fig. 3 Comparison of signal intensity for thermal stability of developed immunosensor

effect of temperature on the immunoassay was evaluated in the range 20 °C to 50 °C and presented as Fig. 3. In both cases i.e., 1° Ab immobilized on plate and 1° Ab immobilized on ZnO-NPs showed similar behavior. However, enhance signal intensity was found in the range 26 °C to 35 °C for the 1° Ab-ZnO-NPs over the 1° Ab immobilized on plate. Above 40 °C, the signal intensity was decreased and reached to the blank value i.e., signal intensity without any pAb-HRP. Thus, all experiments were carried out at 30 °C. So, the 1° Ab on modified ZnO-NPs exhibited good thermal stability compared to the 1° Ab immobilized on polystyrene plate.

Effect of surface modification

The performance of the 1° Ab coupled to the ZnO-NPs was evaluated as against the 1° Ab immobilized on microwell plate using optimized condition. The kinetic intensity profile of the resulting signal intensity was recorded as Fig. 4. The signal reached a stable value (95 % of the steady state) after 25 min for 1° Ab-ZnO-NPs. The stable signal intensity was found at 30 min in case of 1° Ab coated on plate. The covalently attached 1° Ab showed significantly higher signal intensity over the 1° Ab coated on microwells. The order of the stable signal intensity recorded in absence of CEA for 1° Ab functionalized ZnO-NPs was found to be 20600 ADU (via phosphonation) and 6230 ADU for 1° Ab coated on microwells (i.e., non-specifically adsorbed 1° Ab) respectively (n=5) (Inset of Fig. 4). The signal intensities were found to 3 fold higher for phosphonated ZnO-NPs against 1° Ab coated on microwells. These observations were also found true for the inhibition studies. The control over bio-molecule's surface orientation suggests that SAMs played an important role for the construction of immuno recognition surfaces.

Immunoassay for CEA in serum

To evaluate the analytical performance of sensor, calibration was obtained for CEA spiked serum samples under optimized conditions. The inhibition curve for CEA was obtained at different concentrations of CEA in the range 0.001 – 20 ng·mL^{-1} using CL technique. The calibration curves were fitted by using Origin Pro 8 SR0 software. Percentage inhibition (%I) was calculated as described by Arduini et al., [23] in presence and absence of analyte.

$$I\,\% = \frac{I_0 - I_A}{I_0} \times 100 \quad (1)$$

Where, I_0=Signal Intensity of blank; I_A=Signal Intensity of spiked sample

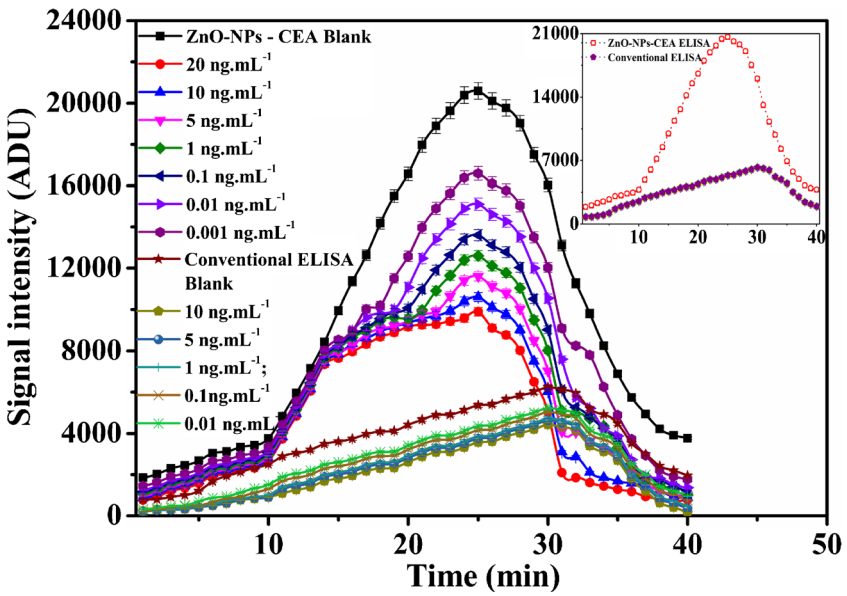

Fig. 4 Comparison of signal intensity under optimized condition between ZnO-NPs-CEA ELISA and conventional microwell plate ELISA for CEA in the range 0.001 – 20 ng mL^{-1}. (Inset: kinetics plot for the both method in absence of CEA)

The percentage of inhibited activity that results after exposure to the CEA is quantitatively related with the inhibitor concentration according to the equation. The limit of detection (LOD) was defined as the lowest concentration of analyte that exhibits a signal of 15 % inhibition [24].

A calibration curve for various CEA concentration (0.001–20 ng·mL^{-1}) is presented as Fig. 5. The calibration was found to be linear in the range 0.001–20 ng·mL^{-1} (R^2=0.982, n=5) with a relative standard deviation (RSD) of 3.21 %±0.83 for the 1° Ab attached through 16-PHA modified ZnO-NPs (Fig. 5). The linear equation was y=7.1574×(ng·mL^{-1})+40.65317. Limit of detection (LOD) was 0.001 ng·mL^{-1} and limit of quantitation (LOQ) was 0.001 ng·mL^{-1} by analyzing replicate sets of modified ZnO-NPs with good sensitivity about 7.86 %. Whereas for conventional polystyrene plate ELISA, the linearity was found in the range 0.01 – 10 ng·mL^{-1} (R^2=0.9692, n=5) with an RSD of 5.17 %±0.69 (Fig. 5). The linear equation was y=4.08864×(ng·mL^{-1})+23.85789. LOD and LOQ were determined as 0.01 ng·mL^{-1} by analyzing replicate sets with very low sensitivity about 3.7 %. Lower LOD, LOQ value, R^2 and sensitivity indicate that a surface-active head group which binds strongly to a substrate, an alkyl chain giving stability to the assembly that plays an important role in terms of coupling of biomolecules to self assembled monolayers. Although the developed immunoassay comprises of three antibodies, however, in view of prognosis of cancer, this method could be a better choice over conventional microplate ELISA (Table 1).

Selectivity, recovery and real sample analysis

The developed immunosensor was studied for its selectivity in the incubation solution with 0.2, 2 and 20 ng·mL^{-1} CEA. The

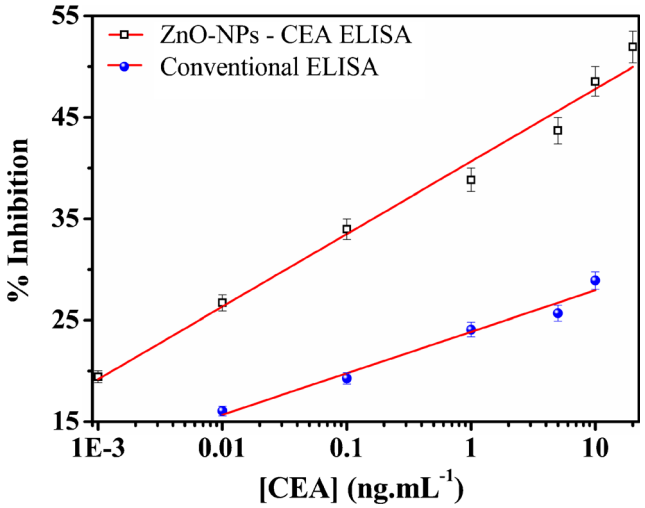

Fig. 5 Calibration curve for various [CEA] using 1° Ab immobilized through 16-PHA SAMs on ZnO-NPs and 1° Ab coated on polystyrene microwell plate under optimized condition (Inset: linear calibration curve)

Table 2 Comparison of real sample analysis using ZnO-NPs – CEA ELISA and conventional ELISA with 1° Ab coated on microwell plate

Technique	Sample-1 (ng·mL^{-1}) Mean±S.D.	Sample-2 (ng·mL^{-1}) Mean±S.D.	Sample-3 (ng·mL^{-1}) Mean±S.D.	Sample-4 (ng·mL^{-1}) Mean±S.D.	Sample-5 (ng·mL^{-1}) Mean±S.D.	Sample-6 (ng·mL^{-1}) Mean±S.D.	Sample-7 (ng·mL^{-1}) Mean±S.D.	Sample-8 (ng·mL^{-1}) Mean±S.D.
ZnO-NPs - 16 PHA –1° Ab	4.25±0.022	1.784±0.0151	7.631±0.14	2.112±0.0042	1.127±0.0722	0.771±0.0565	0.1564±0.0192	3.911±0.0043
on polystyrene microwell plate	4.382±0.0471	1.81±0.064	7.393±0.261	2.091±0.0114	1.133±0.0084	0.753±0.00531	0.1442±0.0163	3.852±0.05182

% I was calculated from the signal intensity values in the presence of the interference and without interference (Supplementary Figure S5, S6 and S7). The results showed that the interferences of relatively high concentrations only posed negligible effects on CEA detection, indicating that the selectivity of the developed immunosensor was acceptable.

The stability of 1° Ab immobilized on ZnO-NPs was assessed over one month period at storage condition 4 °C in 10 mM PBS (pH 7.4). No significant loss in the 1° Ab functional activity was observed even after four weeks (Supplementary Figure S8). The response was found to be superior over microplate sandwich ELISA technique.

Recovery experiments were conducted to evaluate the accuracy and precision of the ZnO-NPs – CEA immunoassay. Known amounts of CEA were spiked to seven serum samples in triplicate. Recovery experiments were performed for both formats. CEA was fortified at levels of 0.01, 0.05, 1, 2.5, 10, 15 and 20 $ng \cdot mL^{-1}$; the recoveries of CEA were found in range 97 to 100 % for ZnO-NPs – CEA immunoassay and 90 to 104 % for microplate ELISA. The results of the accuracy and precision test are listed in Supplementary Table S1.

Further, to demonstrate the applicability of the ZnO-NPs – CEA CL ELISA for the determination of CEA in real serum samples, eight different serum samples were collected. The serum samples were diluted in distilled water (3:7). The results were obtained using both ZnO-NPs – CEA ELISA and microplate ELISA. We found that the results of the ZnO-NPs – CEA ELISA method correlated well with those of the microplate ELISA as shown in Table 2, showing that the ZnO-NPs – CEA ELISA can detect the presence of CEA in serum samples both qualitatively and quantitatively. The correlation between the developed method and the conventional ELISA was plotted. The correlation coefficient (r) was obtained from the graph and as well as calculated theoretically i.e., 0.99998 and 0.999965 respectively (Supplementary Figure S9, S10). This indicates that both methods are highly correlated.

Conclusions

In this endeavor, we have demonstrated an ultrasensitive hybrid sandwich-immunoassay for the determination of CEA in human serum based on functionalized ZnO-NPs. The immunoassay exhibits an excellent analytical performance in terms of linearity, enhanced selectivity over polystyrene microwell-plate conventional ELISA. ZnO-NPs facilitated the catalysis during H_2O_2-luminol reaction, and also the 16-PHA modified ZnO-NPs exhibited an enhanced thermal stability (1.39 fold). The enhancement in CL intensities facilitated improved assay performance in sensitivity and stability. Moreover, the higher isoelectric point of ZnO-NPs than CEA allows toward novel bio – nano interface by immobilizing high amount of capture probes. The developed method showed better selectivity in presence of other interfering elements. The most promising feature of ZnO-NPs – ELISA is the low-cost and high capture efficiency over other reported materials.

References

1. Choi Y-E, Kwak J-W, Park JW (2010) Nanotechnology for early cancer detection. Sensors 10:428–455
2. Cheow LF, Ko SH, Kim SJ, Kang KH, Han J (2010) Increasing the sensitivity of enzyme-linked immunosorbent assay using multiplexed electrokinetic concentrator. Anal Chem 82:3383–3388
3. Qu S, Liu J, Luo J, Huang Y, Shi W, Wang B, Cai X (2013) A rapid and highly sensitive portable chemiluminescent immunosensor of carcinoembryonic antigen based on immunomagnetic separation in human serum. Anal Chim Acta 766:94–99
4. Zhou F, Yuan L, Wang H, Li D, Chen H (2011) Gold nanoparticle layer: a promising platform for ultra-sensitive cancer detection. Langmuir 27:2155–2158
5. Ambrosi A, Airò F, Merkoçi A (2009) Enhanced gold nanoparticle based ELISA for a breast cancer biomarker. Anal Chem 82:1151–1156
6. Pei X, Zhang B, Tang J, Liu B, Lai W, Tang D (2013) Sandwich-type immunosensors and immunoassays exploiting nanostructure labels: a review. Anal Chim Acta 758:1–18
7. Park J-S, Cho MK, Lee EJ, Ahn K-Y, Lee KE, Jung JH, Cho Y, Han S-S, Kim YK, Lee J (2009) A highly sensitive and selective diagnostic assay based on virus nanoparticles. Nat Nanotechnol 4:259–264
8. Wang G, Huang H, Zhang G, Zhang X, Fang B, Wang L (2011) Dual amplification strategy for the fabrication of highly sensitive Interleukin-6 amperometric immunosensor based on poly-dopamine. Langmuir 27:1224–1231
9. Cassiday L (2010) Carbon nanotubes stretch the boundaries of biomarker detection. Anal Chem 82:3406
10. Borras G, Molina R, Xercavins J, Ballesta A, Iglesias J (1995) Tumor antigens CA 19.9, CA 125, and CEA in carcinoma of the uterine cervix. Gynecol Oncol 57:205–211
11. Grunnet M, Sorensen JB (2012) Carcinoembryonic antigen (CEA) as tumor marker in lung cancer. Lung Cancer 76:138–143
12. Hammarström S (1999) The carcinoembryonic antigen (CEA) family: structures, suggested functions and expression in normal and malignant tissues. Semin Cancer Biol 9:67–81
13. Chon H, Lee S, Son SW, Oh CH, Choo J (2009) Highly sensitive immunoassay of lung cancer marker carcinoembryonic antigen using surface-enhanced Raman scattering of hollow gold nanospheres. Anal Chem 81:3029–3034
14. Kulasingam V, Diamandis EP (2008) Strategies for discovering novel cancer biomarkers through utilization of emerging technologies. Nat Clin Pract Oncol 5:588–599
15. Pal S, Sharma MK, Danielsson B, Willander M, Chatterjee R, Bhand S (2014) A miniaturized nanobiosensor for choline analysis. Biosens Bioelectron 54:558–564
16. Solanki PR, Kaushik A, Agrawal VV, Malhotra BD (2011) Nanostructured metal oxide-based biosensors. NPG Asia Mater 3:17–24
17. Vashist SK, Marion Schneider E, Lam E, Hrapovic S, Luong JHT (2014) One-step antibody immobilization-based rapid and highly-sensitive sandwich ELISA procedure for potential in vitro diagnostics. Sci Rep 4:4407

18. Willander M, Khun K, Ibupoto Z (2014) Metal oxide nanosensors using polymeric membranes, enzymes and antibody receptors as ion and molecular recognition elements. Sensors 14:8605–8632
19. Arya SK, Saha S, Ramirez-Vick JE, Gupta V, Bhansali S, Singh SP (2012) Recent advances in ZnO nanostructures and thin films for biosensor applications: Review. Anal Chim Acta 737:1–21
20. Norouzi P, Gupta VK, Faridbod F, Pirali-Hamedani M, Larijani B, Ganjali MR (2011) Carcinoembryonic antigen admittance biosensor based on Au and ZnO nanoparticles using FFT admittance voltammetry. Anal Chem 83:1564–1570
21. Casey BJ, Kofinas P (2008) Selective binding of carcinoembryonic antigen using imprinted polymeric hydrogels. J Biomed Mater Res A 87:359–363
22. Li S-F, Zhang X-M, Du W-X, Ni Y-H, Wei X-W (2008) Chemiluminescence reactions of a luminol system catalyzed by ZnO nanoparticles. J Phys Chem C 113:1046–1051
23. Arduini F, Amine A, Moscone D, Palleschi G (2009) Reversible enzyme inhibition–based biosensors: Applications and analytical improvement through diagnostic inhibition. Anal Lett 42:1258–1293
24. Jiang J, Wang Z, Zhang H, Zhang X, Liu X, Wang S (2011) Monoclonal antibody-based ELISA and colloidal gold immunoassay for detecting 19-Nortestosterone residue in animal tissues. J Agric Food Chem 59:9763–9769
25. Liu N, Feng F, Liu Z, Ma Z (2015) Porous platinum nanoparticles and PdPt nanocages for use in an ultrasensitive immunoelectrode for the simultaneous determination of the tumor markers CEA and AFP. Microchim Acta 182:1143–1151
26. Wu K, Chu C, Ma C, Yang H, Yan M, Ge S, Yu J, Song X (2015) Immunoassay for carcinoembryonic antigen based on the Zn^{2+}-enhanced fluorescence of magnetic-fluorescent nanocomposites. Sensors Actuators B Chem 206:43–49
27. Cheng Y, Yuan R, Chai Y, Niu H, Cao Y, Liu H, Bai L, Yuan Y (2012) Highly sensitive luminol electrochemiluminescence immunosensor based on ZnO nanoparticles and glucose oxidase decorated graphene for cancer biomarker detection. Anal Chim Acta 745:137–142